Development 127, 4443-4453 (2000)
Printed in Great Britain © The Company of Biologists Limited 2000
DEV0333

The *SPIRAL* genes are required for directional control of cell elongation in *Arabidopsis thaliana*

Ikuyo Furutani, Yuko Watanabe, Rafael Prieto, Masatoshi Masukawa, Koya Suzuki, Kuniko Naoi, Siripong Thitamadee, Toshiharu Shikanai and Takashi Hashimoto*

Graduate School of Biological Sciences, Nara Institute of Science and Technology, 8916-5 Takayama, Ikoma 630-0101, Japan
*Author for correspondence (e-mail: hasimoto@bs.aist-nara.ac.jp)

Accepted 9 August; published on WWW 26 September 2000

SUMMARY

Cells at the elongation zone expand longitudinally to form the straight central axis of plant stems, hypocotyls and roots, and transverse cortical microtubule arrays are generally recognized to be important for the anisotropic growth. Recessive mutations in either of two *Arabidopsis thaliana SPIRAL* loci, *SPR1* or *SPR2*, reduce anisotropic growth of endodermal and cortical cells in roots and etiolated hypocotyls, and induce right-handed helical growth in epidermal cell files of these organs. *spr2* mutants additionally show right-handed twisting in petioles and petals. The *spr1spr2* double mutant's phenotype is synergistic, suggesting that SPR1 and SPR2 act on a similar process but in separate pathways in controlling cell elongation. Interestingly, addition of a low dose of either of the microtubule-interacting drugs propyzamide or taxol in the agar medium was found to reduce anisotropic expansion of endodermal and cortical cells at the root elongation zone of wild-type seedlings, resulting in left-handed helical growth. In both *spiral* mutants, exogenous application of these drugs reverted the direction of the epidermal helix, in a dose-dependent manner, from right-handed to left-handed; propyzamide at 1 μM and taxol at 0.2-0.3 μM effectively suppressed the cell elongation defects of *spiral* seedlings. The *spr1* phenotype is more pronounced at low temperatures and is nearly suppressed at high temperatures. Cortical microtubules in elongating epidermal cells of *spr1* roots were arranged in left-handed helical arrays, whereas the highly isotropic cortical cells of etiolated *spr1* hypocotyls showed microtubule arrays with irregular orientations. We propose that a microtubule-dependent process and SPR1/SPR2 act antagonistically to control directional cell elongation by preventing elongating cells from potential twisting. Our model may have implicit bearing on the circumnutation mechanism.

Key words: Anisotropic growth, *Arabidopsis thaliana*, Circumnutation, Microtubule, Propyzamide, Taxol

INTRODUCTION

There are numerous examples of left-right asymmetries in biological systems. Although the development of left-right asymmetries in vertebrates recently began to yield to molecular analysis (Capdevila et al., 2000), cellular and molecular mechanisms of handedness in plants have not been explored at all. Many species of twining plants show apparent handedness, either consistently forming right- or left-handed helices as they climb. Here, the direction of a helix is defined as right-handed when it matches the appearance of a right-handed corkscrew. For example, runner bean and bindweed make right-handed helices, whereas hop and honeysuckle produce left-handed helices (Coen, 1999). Helical growth is not restricted to tendrils of climbing plants. Darwin surveyed dozens of plant species and discovered that oscillating growth of plant organs is widespread and introduced the term 'circumnutation' (Darwin, 1875; Darwin and Darwin, 1880). Roots, hypocotyls, shoots, branches and flower stalks may oscillate either in a clockwise or anticlockwise direction, strictly in a growth-dependent manner. More recently circumnutations have been found not only in dicots and monocots but also in gymnosperms, fungi and algae (Brown, 1993). A 'wavy' growth pattern of *Arabidopsis thaliana* roots on inclined agar plates (Okada and Shimura, 1990) is also interpreted to result from circumnutation and gravitropism (Simmons et al., 1995). Although much descriptive work has been carried out for several decades to characterize the kinematics of circumnutations, models describing the underlying mechanisms remain speculative.

There are further examples of handedness in plants. The petals of several species are arranged like fan blades that all seem to twist in the same direction, forming either a clockwise or an anticlockwise appearance. Clockwise-rotating petals are found, for example, in oleander, whereas petals of the greater periwinkle are arranged in an anticlockwise fashion (Coen, 1999). Plant species of the families Guttiferae, Malvaceae and Oxalidaceae, however, generally develop clockwise- and anticlockwise-rotating flowers with equal frequency. Therefore, either a chance event or a genetically determined developmental program appears to produce flowers with distinct handedness.

The patterned arrangement of organs such as leaves around the shoot axis (phyllotaxy) represents another example of handedness in plants. A spiral/helical phyllotactic pattern where leaves are formed 137.5° apart predominates in nature (Williams, 1975). In *Arabidopsis thaliana*, the handedness of the generative spiral is maintained throughout vegetative development and can be either clockwise or anticlockwise in equal frequency (Callos and Medford, 1994). This stochastic phyllotactic handedness can be traced back to the asymmetry in the developmental distances between the two cotyledons during *Arabidopsis* embryo development (Woodrick et al., 2000).

Genetically controlled handedness should be amenable to molecular genetic studies. In this study, we have screened *Arabidopsis thaliana* seedlings for mutants with consistent right-handed skewing of root epidermal cell files. Furthermore, we have also found that treatment of seedlings with drugs that compromise microtubule (MT) functions produces a left-handed helical growth. We propose a model in which anisotropic growth is controlled by antagonizing effects between a MT-organizing process and *SPR* genes.

MATERIALS AND METHODS

Plant growth conditions, plant strains and genetic crosses

Arabidopsis thaliana seeds were sterilized in 5% sodium hypochlorite and were allowed to germinate on plates containing 0.5× *Arabidopsis* nutrient solution (Haughn and Somerville, 1986), 2% sucrose and 1.5% agar, unless otherwise noted. After 2 days at 4°C, plates were incubated in a near vertical position at 22°C with a 16 hour light/8 hour dark cycle, unless otherwise noted. Day 0 of growth is defined as the time when plates were transferred to 22°C. To prepare stock solutions, oryzalin (AccuStandard, New Haven, CT), propyzamide (Wako, Osaka, Japan), and taxol (Nacalai tesque, Kyoto, Japan) were dissolved in dimethyl sulfoxide. Final concentrations of dimethyl sulfoxide in the media were lower than 0.3%, at which concentration the growth of seedlings was not affected.

The *spr1-1* and *spr2-1* mutant alleles were isolated from fast-neutron mutagenized M2 seeds of the Landsberg *erecta* (Ler) ecotype (Lehle Seeds, Round Rock, TX), whereas *spr1-4* was recovered from gamma-ray mutagenized M2 seeds of the Wassilewskija ecotype (Lehle Seeds). *spr1-2* and *spr1-3* in the Columbia background were isolated, respectively, by J. Schiefelbein from enhancer trap lines produced by T. Jack (ABRC stock center), and by K. Nakamura from fast-neutron mutagenized M2 seeds (Lehle Seeds). *tortifolia1* (Enkheim ecotype) was obtained from T. Schäffner, and *convoluta* (S95 ecotype) was obtained from ABRC stock center. *spr1-1* and *spr2-1* alleles were out-crossed at least three times and twice, respectively, to the Ler wild type before being used in this study.

For mapping, homozygous *spr1-1* and *spr2-1* plants were crossed with Col wild-type plants, and selfed to give F_2-mapping populations. Seedlings homozygous for the *spr* mutation were selected and used to extract DNA for mapping with CAPS and SSLP markers (http://www.arabidopsis.org/aboutcaps.html).

The *spr1-1spr2-1* double mutant was selected in F_2 populations, and the homozygous double mutants in the F_3 generation were used for phenotypic analysis. Spiral phenotypes in root, petiole and hypocotyl were used to distinguish the *spr1-1* and *spr2-1* mutations. A 0.6-kb deletion in the *SPR1* gene was also used to confirm the *spr1-1* mutation by genomic PCR (I. F., H. Tachimoto and T. H., unpublished).

Phenotypic analysis

Spiral phenotypes of whole seedlings were analyzed using an Olympus stereoscope SZX12 equipped with an Olympus digital camera DP10. For measurement of length and width of root cells, seven-day-old seedlings grown at 22°C were cleared with chloral hydrate, and viewed under Nomarski optics. Optical sections of root cells at the differentiation zone were made at a series of focal planes, and the maximal cell width of epidermis, cortex and endodermis was determined. Distance from the quiescent center, cell length and skewed angle of the long cell axis from the central axis of a primary root were likewise measured on the root epidermal cells of ten-day-old seedlings grown at 14°C.

For histological analysis, hypocotyls of five-day-old etiolated seedlings were fixed and embedded in Technovit 7100 (Kulzer, Hereaus), essentially as described (Scheres et al., 1994). A series of 6 μm thick logitudinal sections and 8 μm thick transverse sections were made with a rotary microtome HM325 (Microm). Transverse sections were serially aligned from the shoot tip to the rapidly elongating region (approximately 1 mm away from the tip), so that the distance from the tip could be assigned for given sections. Sections were stained with toluidine blue O and photographed on an Olympus BX50 microscope equipped with a PM-20 camera.

Replica images of seedlings were made using polyvinylsiloxane impression material (Extrude; Keer Co., Romulus, MI) and epoxy glue (Araldite; Ciba Geigy), coated with Pt, and examined with scanning electron microscopy N3200 (Hitachi).

Immunolabeling procedure

The protocol for fixing and immunostaining of seedling roots was as described (Wasteneys et al., 1998; Sugimoto, 2000 – PhD Thesis, The Australian National University.) except that the cold methanol treatment was not used and we used anti-α-tubulin (N356; Amersham) diluted 1:1000 in wash buffer as a primary antibody.

Hypocotyls of five-day-old etiolated seedlings were fixed, rinsed and embedded in 5% agar. Fixed hypocotyls in the agar blocks were cut longitudinally into 100 μm thick sections with a DTK-1500 microslicer (Dohan EM, Kyoto, Japan). Buffers, fixation solutions and immunolabeling procedures were the same as those used for roots.

Evaluation of MT arrays

Stained cells were optically sectioned at several different focal planes with a confocal laser-scanning microscope LSM510 (Zeiss). The orientation of cortical MTs adjacent to the outer tangential wall of each epidermal cell was measured at upper, middle and lower regions of the longest cell axis with an image processing software MacSCOPE (Mitani, Fukui, Japan), and the three measurements were averaged to represent the MT angle of the examined cell. In a majority of epidermal cells, the orientation of cortical MTs was uniform within the cell.

RESULTS

Isolation of *spr* mutants

When wild-type *Arabidopsis thaliana* seedlings (Ler ecotype) were grown vertically on a hard-agar surface, the direction of root growth deviated slightly to the left of vertical (when the seedlings are viewed from above the agar surface; Fig. 1A). The *spiral* (*spr*) mutants were isolated primarily on the basis of their tendency to bend to the right (Fig. 1A). After test crosses, these mutants were classified into two non-complementation groups. We identified four alleles of *spr1* (*spr1-1* to *spr1-4*), and one allele of *spr2* (*spr2-1*). The phenotypic similarity of *spr2* to previously reported mutants prompted us to conduct complementation tests between them, which revealed that *spr2* is allelic to *tortifolia1* (Bürger, 1971) and *convoluta* (Relichova, 1976). A pleiotropic arabidopsis

mutant that partially resembles *spr* mutants and was interpreted to result from two independent mutations was also reported (Marinelli et al., 1997), but was not tested here for the allelism. Upon outcrossing the *spr* alleles to wild type, all F1 seedlings were phenotypically wild-type, and the F1 plants produced 25% mutant seedlings upon selfing, indicating that *spr1* and *spr2* mutations are recessive.

Mapping against molecular markers in a mapping population of F2 *spr* seedlings revealed that *SPR1* is tightly linked to m246 on the top of chromosome 2 (no recombination among 282 chromosomes), and that *SPR2* is positioned 0.27 cM south of PG11 and 1.5 cM north of mi123 on chromosome 4, in accordance with linkage of *TORTIFOLIA1* to *cer2* and d104 in that region (Fabri and Schäffner, 1994).

spr phenotype

Since all four *spr1* alleles showed very similar phenotypes, the *spr1-1* allele was characterized in detail although the results obtained were essentially reproduced in the *spr1-2* allele. When grown on a vertically positioned hard-agar surface, *spr1-1* seedling roots grew sharply skewed to the right, while *spr2* roots grew almost vertically or slightly skewed to the right (Fig. 1A). Under these conditions, both *spr* roots showed typical wavy growth paths as observed in wild-type roots. The *spr1* root meristem appeared normal but, at the distal elongation zone, epidermal cell files formed right-handed helices (Fig. 1C). The right-handed helix extended from the differentiation zone to the base of the primary root, and was observed in the lateral roots as well. Physical contact with the agar surface did not affect the helical phenotype since the *spr1* roots projecting into the air or growing within the agar also showed the constitutive helical epidermis (not shown). When *spr1* roots penetrated the agar, the submerged roots grew directly downwards (Fig. 1F), indicating that the skewing to the right on the hard agar surface was caused by right-handed torsion at the root tip generated by the constitutive right-handed helix of *spr1* epidermal cell. The helical epidermal cell files were not apparent in wild-type and *spr2* roots (Fig. 1B,D).

When grown in white light, hypocotyls of wild-type and *spr1* seedlings were indistinguishable, whereas the epidermal cell files of *spr2* hypocotyl skewed slightly to the right (Fig. 2A-C). The cotyledon petioles showed right-handed skewing in *spr2*, resulting in anticlockwise rotation of cotyledons when plants were viewed from above the plate (see Fig. 6D). It is known that dark-grown hypocotyls after 3 days growth elongate at the basal-mid regions, and that the elongation zone moves up the hypocotyl with time; at day 5, the apical third of the hypocotyl is rapidly elongating (Gendreau et al., 1997). We therefore examined etiolated hypocotyls at day 3 and day 5. The epidermal cell files of three-day-old dark-grown *spr1* and *spr2* hypocotyls skewed to the right, especially at the basal-mid regions (Fig. 2F,G). When the seedlings were grown for a further 2 days in the dark, epidermal skewing strongly intensified at the apical one-third of the *spr1* hypocotyl (Fig. 2J,N), whereas no such enhancement was observed in *spr2* (Fig. 2K,O).

Vegetative and reproductive development of *spr1* and *spr2* plants were mostly normal, and these plants were fully fertile. In *spr2*, rosette leaves and petals showed anticlockwise twisting (Fig. 3C,G), and cauline leaves also tended to curl in an anticlockwise direction (not shown). While inflorescence

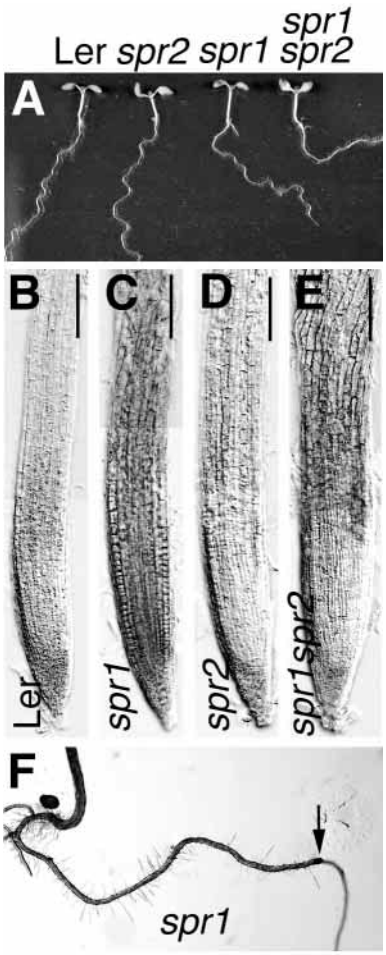

Fig. 1. Phenotype of seedlings grown on a vertically positioned agar plate for 7 days in white light. (A) The Ler seedling root grows slightly skewed to the left, whereas the roots of *spr2-1*, *spr1-1* and the double mutant grow to the right, in increasingly sharp angles. Petioles of *spr2-1* and the double mutant also twist in a clockwise direction. (B-E) Epidermal cell files of *spr1-1* (C) and *spr1spr2* (E) skew to the right at the distal elongation zone, whereas cell files of Ler (B) and *spr2-1* (D) appear straight. (F) A *spr1-1* root grows to the right on the agar but, in the event of its growth through the agar (arrow), it bends and continues to grow vertically. Scale bars: 100 μm.

stems of light-grown *spr* mutants looked the same as wild type, those of dark-grown plants had right-handed helices in epidermal cell files; the epidermal defect was especially strong in *spr1* plants (not shown). In general, the *spr1* twisting phenotype is stronger in dark-grown central axis, including stem, hypocotyl and root, whereas *spr2* phenotype is most apparent in lateral appendages, such as petioles, cauline leaves and petals.

The *spr1-1spr2-1* double mutant showed strong synergistic defects in all aspects of the *spr1* and *spr2* phenotypes. The *spr1spr2* seedling root was shorter and wider, grew more strongly skewed to the right when grown on the agar and had epidermal cell files that skewed more strongly to the right than expected from simple addition of the *spr1* and *spr2* phenotypes (Fig. 1A,E). The hypocotyl epidermis of light-grown *spr1spr2* seedlings also showed right-handed helix more strongly

skewed than the light-grown *spr2* hypocotyl epidermis, and included many deformed cells (Fig. 2D). Hypocotyls of etiolated double mutant seedlings were much shorter than those of either parental mutants (Fig. 2H,L), and consisted of round epidermal cells with highly reduced anisotropic growth in the upper hypocotyl region (Fig. 2P). Characteristic protrusions or bumps were often observed at the central region of the expanded epidermal cells in both light- and dark-grown hypocotyls (arrowheads in Fig. 2D,P). Rosette leaves of *spr1spr2* plants were smaller than the leaves of either parental plants (Fig. 3D).

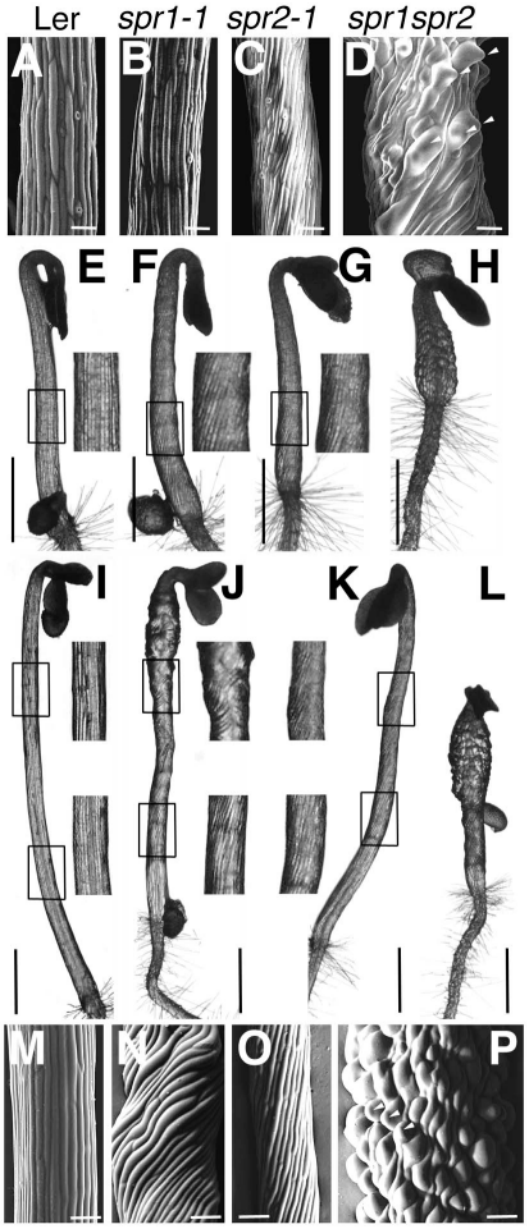

Fig. 2. Helical growth phenotype of hypocotyls. (A-D) Scanning electron micrograph of upper hypocotyl regions of 7-day-old light-grown seedlings. (E-H) 3-day-old etiolated seedlings. (I-L) 5-day-old etiolated seedlings. (M-P) Scanning electron micrograph of upper hypocotyl regions of 5-day-old etiolated seedlings. (A,E, I,M) Ler, (B,F,J,N) *spr1-1*, (C,G,K,O) *spr2-1* and (D,H,L,P) *spr1-1spr2-1*. Insets in E-G and I-K are enlarged twice from the regions indicated by boxes. Arrowheads indicate some of the local bulges on the epidermal cells. Scale bars: 100 μm in A-D,M-P; 1 mm in E-L.

Cell anisotropy

To address cellular defects in *spr* mutants, longitudinal and transverse sections of plastic-embedded seedlings were made at the upper region of etiolated hypocotyls (Fig. 4). The longitudinal sections that cut hypocotyls just at their mid planes (Fig. 4A-D) were used to measure the distance of each cell in the inner cortex cell file from the shoot apex (Fig. 5). Inner cortex cells of wild-type hypocotyls gradually elongated as the distance from the shoot apex increased, and became much longer, starting from the fifth cortex cell approximately 450 μm distal from the apex. Inner cortex cells of *spr1*, *spr2* hypocotyls elongated at wild-type rates up to the fifth cortex cells, but thereafter did not keep up with the progressively faster elongation; the elongation defect was more pronounced in *spr1* than in *spr2*. Inner cortex cells of *spr1spr2* hypocotyls expanded even more slowly than *spr1* or *spr2* rates in the longitudinal direction.

Inner and outer cortex cells of etiolated wild-type hypocotyls were polyhedral in transverse section (Fig. 4A,F). The shape of individual cells was more or less uniform within each cell layer of ground tissue (endodermis and two cortex layers), and this stereotypical cell arrangement continued from the shoot apical region to the basal region. The transverse sections of *spr1* hypocotyls up to approximately 400 μm distal from the apex looked the same as wild type, although a few cells in each ground tissue layer were occasionally somewhat enlarged (not shown). Cell expansion was clearly abnormal in *spr1* hypocotyls at the region starting approximately 500 μm distal from the apex (Fig. 4B), which corresponds to the fifth cell from the apex (Fig. 5). A series of transverse sections from 600 μm to 680 μm (Fig. 4H-I), combined with longitudinal sectioning analysis (Fig. 4B), showed that the cells in ground tissue were only weakly elongated. The same sections also showed that the *spr1* cells in epidermis and stele kept substantially normal appearance, compared with the ground tissue cells. In *spr2* hypocotyls, there was no clear difference in cell shape and arrangement up to approximately 400 μm, but the shape of cortex cells became somewhat irregular starting approximately 600 μm from the apex (Fig. 4J). In the *spr1spr2* double mutant, the defect in anisotropic expansion was stronger in ground tissue than it was in the parental mutants while epidermal and stele tissues remained relatively normal in appearance (Fig. 4D; transverse sections not shown).

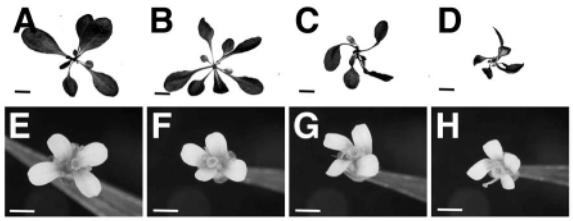

Fig. 3. Phenotype of 2-month-old plants. (A-D) Rosette leaves. (E-H) Flowers. (A,E) Ler, (B,F) *spr1-1*, (C,G) *spr2-1* and (D,H) *spr1-1spr2-1*. Scale bars: 1 cm A-D; 1 mm E-H.

MT-interacting drugs

Interestingly, we found that the addition of a MT-depolymerizing drug propyzamide at 3 μM in the agar medium induced a left-handed helical growth to the epidermal cell files of light-grown wild-type seedling roots and petioles, resulting in root growth skewed to the left and a clockwise twisting of cotyledons (Fig. 6A,E). Etiolated wild-type hypocotyls were more sensitive to propyzamide; 3 μM propyzamide inhibited cell elongation and produced distorted epidermal cell expansion (not shown). In light-grown *spr1* and *spr2* seedlings, propyzamide at 3 μM reversed the direction of helical epidermal cell files from right-handed to left-handed, resulting in root growth skewed to the left on agar plates and a clockwise twisting of cotyledons, as in similarly treated wild-type seedlings (Fig. 6A,F,G). Thus, propyzamide-induced left-handed helical growth is dominant over right-handed helical growth of *spr1* and *spr2*.

We quantified the concentration-dependent effects of propyzamide on the angle of root bending, root length and the direction of cotyledon twisting in light-grown seedlings (Fig. 7A). Propyzamide up to 0.3 μM did not affect wild-type seedlings on the three characteristics examined; 1 μM propyzamide exaggerated slightly the tropic movement of roots to the left; and 3 μM propyzamide induced a clockwise twisting of cotyledons and a strong left-handed helical growth of roots with a concomitant decrease in root length. *spr1* seedlings responded to as low a concentration of propyzamide as 0.1 μM. In a concentration-dependent manner, the rightward bending of *spr1* roots was decreased and at 3 μM a strong left-handed helical growth was observed. In etiolated hypocotyls of *spr1*, 1 μM propyzamide completely suppressed helical growth of epidermal cell files and the highly isotropic expansion of endodermis and cortex cells (compare panels B and E; and panels G-I and K, in Fig. 4). For *spr2*, roots gradually reversed their bending direction from right to left in response to increasing concentrations of propyamide, but even at 3 μM, the leftward bending was not as pronounced as in wild-type or *spr1* roots, indicating that *spr2* roots had reduced responsiveness to propyzamide in this assay. Cotyledon twisting in light-grown *spr2* seedlings and the helical epidermis in etiolated *spr2* were suppressed by 1 μM propyzamide. Oryzalin, another class of MT-depolymerizing drug, also decreased the degree of right-handed helical growth of *spr1* and *spr2* seedling roots when tested up to 0.1 μM (not shown). However, oryzalin at concentrations above 0.1 μM significantly inhibited seedling growth, and complete reversal of helical handedness in *spr* roots and petioles was not attained with this drug.

The MT-stabilizing drug taxol (paclitaxel) was also tested (Fig. 7B). In wild-type seedlings, 0.3 μM taxol had no effect on root helical growth but induced a clockwise twisting of cotyledons (Fig. 6H), and 1 μM taxol induced a strong left-handed bending and reduced root growth. Reduced bending of *spr1* roots was already apparent with 0.3 μM taxol. *spr2* roots responded similarly to increasing concentrations of taxol, although their response to taxol appeared to be more sensitive than the wild-type response. Petiole elongation was inhibited more severely by 1 μM taxol in *spr2* seedlings (Fig. 6J) than in wild-type (Fig. 6H) or *spr1* (Fig. 6I) seedlings. In etiolated seedlings, the strong right-handed helix of *spr1* hypocotyls was suppressed at 0.3 μM taxol, and the weak right-handed helix of *spr2* hypocotyls reversed to a weak left-handed helix at 0.2 μM taxol.

The effects of propyzamide on anisotropic cell expansion were quantified in different root cell layers of light-grown seedlings (Fig. 7C). In wild type, anisotropic cell growth was not affected by 1 μM propyzamide, whereas radial cell expansion in ground tissue, but not in the epidermis, was promoted by 3 μM propyzamide. Anisotropic cell growth, normally impaired in ground tissue of *spr1*, completely recovered to wild-type levels at 1 μM. A higher concentration (3 μM), which induced left-handed helical growth, caused radial cell expansion of ground tissue, but not of the epidermis, in *spr1* roots. In *spr2* roots, defective anisotropic cell expansion of the ground tissue was marginal in the absence of the drug or at 1 μM. Propyzamide at 3 μM induced only weak radial cell expansion of ground tissue.

The cellulose biosynthesis inhibitor 2,6-dichlorobenzonitrile and the actin filament disrupting drug cytochalasin D were tested at low concentrations up to levels that significantly inhibited seedling growth, but neither drug induced helical growth of wild-type seedlings nor did they affect the skewing phenotype of *spr1* and *spr2* seedlings.

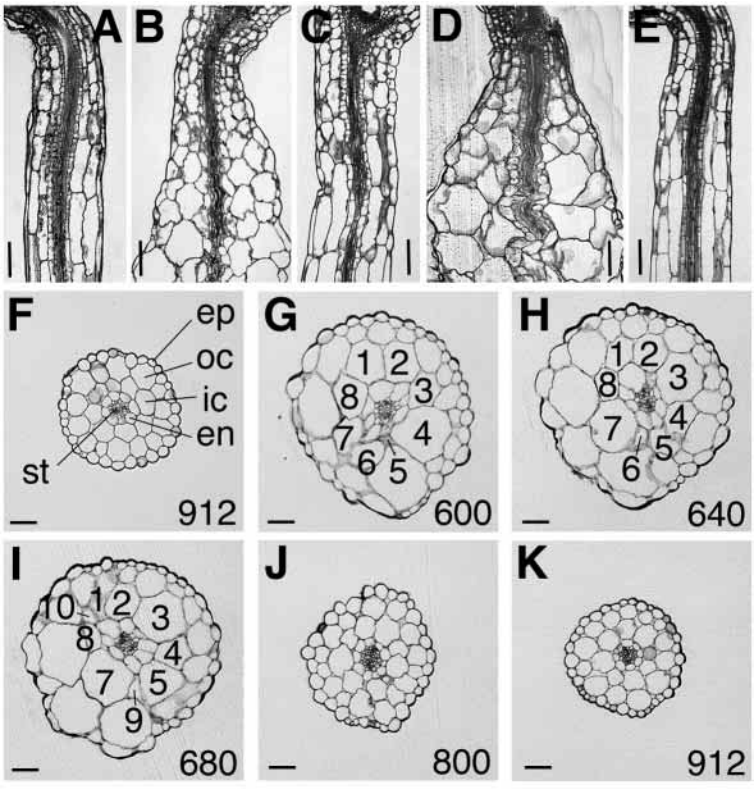

Fig. 4. Sections of upper hypocotyl regions of 5-day-old etiolated seedlings. (A-E) Longitudinal sections. (F-K) Cross sections. Distance from the shoot apex is shown at the lower right corner in μm. Inner cortex cells in G-I are numbered. (A,F) Ler, (B,G-I) *spr1-1*, (C,J) *spr2-1*, (D) *spr1-1spr2-1* and (E, K) *spr1-1* grown in the presence of 1 μM propyzamide. Scale bars: 100 μm in A-E; 50 μm in F-K.

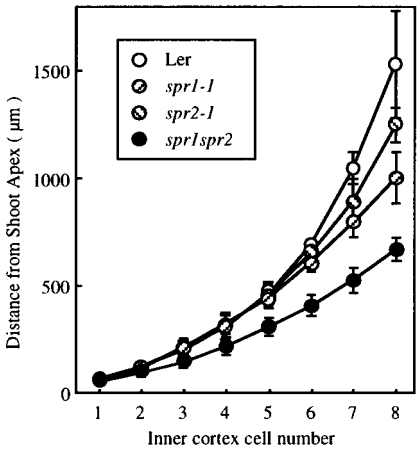

Fig. 5. Distance of inner cortex cells from the shoot tip. Inner cortex cells were counted in files starting at the junction of petiole and hypocotyl procambia and continuing towards the hypocotyl basal regions. Distance was measured between the procambium junction and the center of a given inner cortex cell. More than 20 cortex cell files were measured on longitudinal sections that cut through the middle of vascular cylinders.

Temperature

Although *spr1* leaves usually do not twist when grown at 22°C, we noticed that they often twisted in an anticlockwise direction when grown in a greenhouse during winter. We, therefore, examined the effect of temperature on the skewing phenotype. Epidermal cell files in the upper hypocotyl of etiolated *spr1* seedlings, although skewed at 22°C, were nearly straight at 29°C (Fig. 8B), whereas at 15°C the hypocotyl was short with an exaggerated helical growth (Fig. 8E). Prolonged incubation in the dark at 4°C produced extensive outgrowth of *spr1* hypocotyl epidermal cells, forming abundant hair-like protrusions in the upper hypocotyl region (Fig. 8G). The helical growth of *spr2* hypocotyls, however, was not affected by shifting the growth temperature between 29°C and 15°C (Fig. 8C,F), although at 4°C, etiolated *spr2* hypocotyls occasionally produced similar hair-like protrusions (not shown). *spr1* roots grew slightly to the right at 29°C, bent even more to the right when the temperature was shifted down to 22°C, and then returned to the weak rightward growth when the temperature was shifted back to 29°C (Fig. 8H). Similar temperature-dependency was not observed in *spr2* roots.

Cortical MT arrays

Reduced growth anisotropy and the effects of MT-interacting drugs in *spr* mutants prompted us to examine cortical MT arrays. First, whole-mount MTs of seedling roots grown at 22°C were stained using immunocytochemistry. The method used stained MTs of root epidermal cells from the root apex to the distal end of elongation zone; differentiated root cells rarely stained. Cortical MTs underneath the outer tangential wall were examined in root epidermal cells at the end of elongation

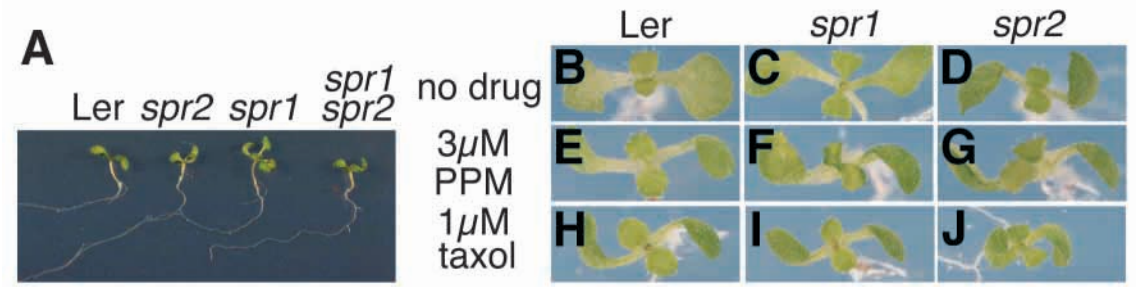

Fig. 6. Effects of propyzamide and taxol on helical growth phenotypes of 7-day-old seedlings grown in the light. (A) Seedlings were grown on agar medium containing 3 μM propyzamide. Seven-day-old seedlings grown on a control medium (B-D), 3 μM propyzamide (PPM) medium (E-G), or 1 μM taxol medium (H-J).

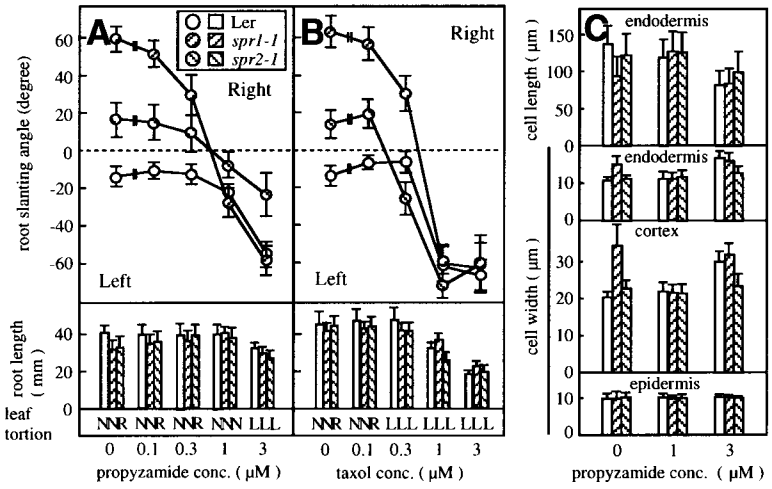

Fig. 7. Effects of propyzamide and taxol on helical growth phenotypes of 7-day-old seedlings grown in the light. (A,B) The angle of root tip deviation from the vertical axis, the root length and the direction of petiole torsion. N, no torsion; R, right-handed; L, left-handed. More than 20 seedlings were measured for each treatment and genotype. (C) Cell length and width of root cells. Root cells in whole-mount preparations were viewed with Nomarski optics and cell sizes measured. More than 50 cells of each cell type were measured for each propyzamide concentration and genotype.

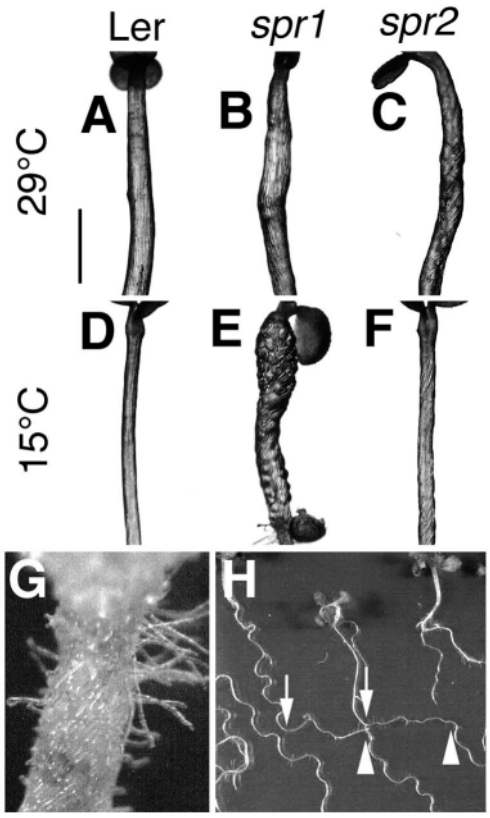

Fig. 8. Temperature sensitivity of helical growth phenotypes. (A-C) Etiolated seedlings grown at 29°C for 5 days. (D-F) Etiolated seedlings grown at 15°C for 10 days. (A,D) Ler, (B,E) *spr1-1* and (C,F) *spr2-1*. (G) Upper hypocotyl region of an etiolated *spr1-1* seedling grown at 4°C for 3 months. Note hair-like protrusions. (H) After being grown at 29°C for 5 days, *spr1-1* seedlings were transferred to 22°C (arrows mark the positions of root tips at the time of transfer). After 2 days, the growth temperature was shifted up to 29°C (arrowheads). Scale bar, 1 mm in A-F.

zone where, in *spr1* and drug-treated wild-type roots, epidermal cell files were already skewed (Fig. 9A,B,D,E). Wild-type cells had cortical MT arrays that were aligned almost transverse to the long axis of the cell (Fig. 9A), while the arrays in *spr1* epidermis were oblique (Fig. 9B). The MT arrays underneath the inner wall of the same cell as in Fig. 9B showed an oblique alignment of opposite slant (Fig. 9C), indicating that the cortical MTs in *spr1* epidermis form left-handed helical arrays. In contrast, wild-type roots treated with 1 μM taxol had right-handed helical arrays (Fig. 9D). Wild-type root cells treated with 3 μM propyzamide had mostly transversely oriented cortical MTs, but occasionally included arrays with right-handed helices (Fig. 9E). In *spr2* roots, the cortical MT arrays appeared to be transverse as in wild-type roots (not shown).

Next, the seedling roots were grown at 14°C, and both the length and angle relative to the long axis of primary root of epidermal cells were plotted with respect to the distance from the quiescent center (Fig. 10A). At 14°C, *spr1* showed an exaggerated phenotype and we could observe clear differences in MT organization between wild type and *spr1,* even in the early phase of cell elongation. Wild-type epidermal cell lengths increased up to approximately 1.2 mm from the quiescent center. *spr1* epidermal cell lengths continued to increase similarly, at least by 0.6 mm, although considerable skewing of *spr1* epidermis prevented accurate measurements beyond this distance (Fig. 10B). Wild-type epidermal cells were aligned essentially parallel to the long axis of primary root, whereas *spr1* cells began to skew to the right starting 550 μm distal to the quiescent center. Thereafter, the skewing angle remained at approximately 20° to the right (Fig. 10C). The orientation of cortical MTs underneath the outer tangential wall was examined in the root epidermal cells positioned between 200 μm and 600 μm from the quiescent center. This region defines the early elongation zone and marginally precedes the helical growth in *spr1*. Cortical MT arrays in wild type were positioned transverse to the long axis of the cell (Fig. 10D). In *spr1*, deviation of the helical pitch was wider and shifted 13° on average from the transverse axis of cells to form left-handed helices (Fig. 10E).

Finally, inner cortex cells were examined at the upper region of etiolated hypocotyls. Wild-type cortex cells were expanding anisotropically and had cortical MTs aligned at right angles to the long axis of the cell (Fig. 9F). In contrast, the orientation of cortical MT arrays was irregular in *spr1* cortex cells with highly reduced anisotropic growth (Fig. 9G,H). The arrays were often parallel in localized regions of a cell, but most cells contained a mixed population of longitudinal, transverse and oblique arrays.

DISCUSSION

Reduced anisotropic cell expansion in ground tissue causes helical epidermal cell files

Since helical growth phenotypes in *spr* mutants and drug-treated seedlings are remarkably similar (though of opposite handedness), we discuss the phenomena collectively. Root and shoot meristems appear to be normal in skewing seedlings. Helical epidermal cell files and the cell elongation defect in ground tissue develop concomitantly at the mid/basal elongation zone where the elongation rate of root (Beemster and Baskin, 1998) and etiolated hypocotyl (Gendreau et al., 1997) becomes progressively accelerated compared with a more apical region. The growth-rate dependency of the helical phenotype is most apparent in the hypocotyls of five-day-old dark-grown *spr1* seedlings, which showed most severe mutant phenotype in the upper quarter of the hypocotyl – the region of most rapid growth (Gendreau et al., 1997). Moreover, helical epidermal cell files in the elongation zone accompany the reduced length of the skewing organs.

Beneath the helical epidermal cell files of the *spr* mutants, cells in ground tissue are more or less isodiametric. This was most obvious in dark-grown *spr1* hypocotyls. In the epidermis, cell files were skewed but radial expansion was scarcely observed. Thus, anisotropic growth of ground tissue is more severely affected than that of epidermal cells in skewing tissues. Taken together with the fact that the skewing angle of cell files progressively decreases from the epidermis through the inner cell layers, reduced anisotropic growth in ground tissue may be the primary cause of helical cell files in the epidermis (Fig. 11A). According to this model, radially expanding ground tissue cell files are shorter along the

longitudinal axis than normally elongating epidermal cell files. Since extra cell production is apparently not induced in ground tissue, the outer cell layers must be skewed to reduce the length along the longitudinal axis to a level comparable with that of the inner cells.

A defect in MT organization may underlie reduced anisotropic growth

Considerable evidence indicates that in most plant cells elongating with polar diffuse growth, the cortical MTs are involved in the orientation of cellulose microfibrils during the synthesis of new cell walls (Giddings and Staehelin, 1991), and thus are essential for establishing the polarity of cell elongation. Several compounds are known to affect polymerization of plant MTs. Propyzamide (also known as pronamide) and oryzalin, two structurally different classes of herbicides, are thought to bind tubulin and promote depolymerization of MTs (Morejohn, 1991), whereas taxol binds the β-tubulin subunit and stabilizes MTs (Bokros et al., 1993). When applied to intact plants at concentrations above certain thresholds, these drugs severely inhibit shoot and root growth, and cause extensive radial swelling in some types of treated cells; however, helical epidermal cell files have not been documented (Morejohn, 1991; Baskin et al., 1994; Hasenstein et al., 1999; and references cited therein). At the drug concentrations used in these and previous studies, cortical MTs are often disorganized, fragmented or depleted by treatment with depolymerizing drugs, or are bundled by taxol treatment. We also observed similar defects in MT organization and radial swelling of root epidermal cells at the propyzamide concentrations much higher than those reported in this study (I. F. and T. H., unpublished). Instead, propyzamide at 3 μM and taxol at 1 μM induced rather weak right-handed helices on the MT arrays in root epidermal cells but the arrays otherwise appeared to be normal. At these relatively low and possibly crucial concentrations, ground tissue might be more sensitive to the drugs than epidermis with regard to the integrity of MT organization and anisotropic growth. In etiolated *spr1* hypocotyls, cortical MT arrays are more irregularly oriented in cortex cells than in epidermal cells, reflecting differential radial swelling between the two cell types. Distinct arrangement or responses of cortical MTs in different cell types have been sporadically noted, such as in cortex and epidermis of oryzalin-treated maize roots (Hasenstein et al., 1999), and in several cell types of cold-treated and untreated maize roots (Baluska et al., 1992, 1993).

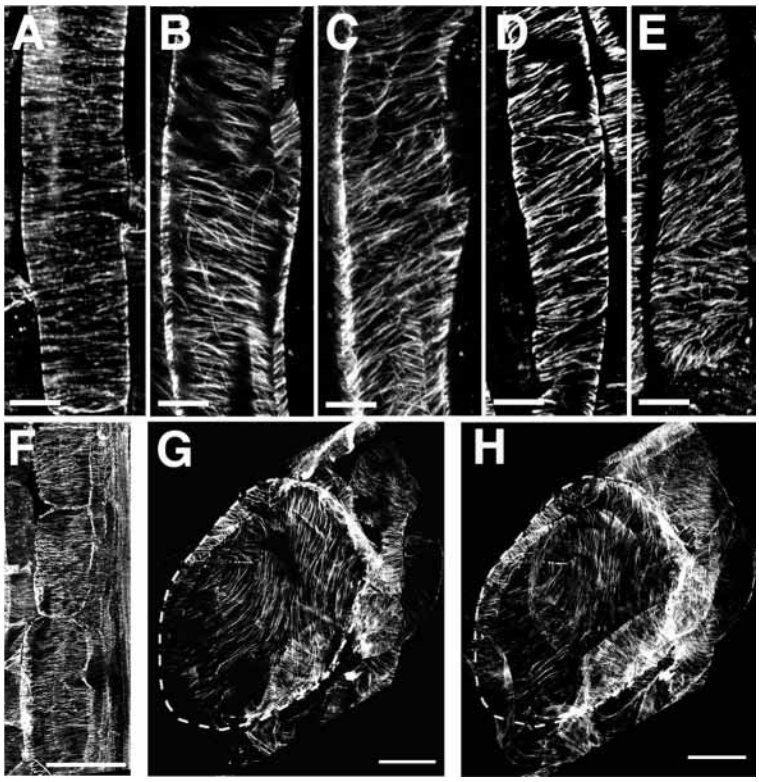

Fig. 9. Micrographs of cortical MTs in seedlings grown at 23°C. (A-E) Root epidermal cells at the basal elongation zone. (A) Ler, (B, C) *spr1-1*, (D) Ler grown on 1 μM taxol and (E) Ler grown on 3 μM propyzamide. Cortical MT arrays were located underneath the outer cell wall (A,B,D,E) or the inner cell wall (C). Panels B and C were from the same *spr1* cell. (F-H) Inner cortex cells at the upper region of 5-day-old etiolated hypocotyls. (F) Ler, and (G,H) *spr1-1*. G and H were from the same *spr1* hypocotyl optically sectioned at different focal planes. Broken line indicates shape of a cell in G and H. All images are positioned in their correct orientation relative to the long axis of the organ. Scale bars, 10 μm in A-E; 50 μm in F-H.

Propyzamide and taxol caused helical growth of identical handedness in arabidopsis seedlings, despite their opposite effects on MT polymerization. At the concentrations effective for inducing helical growth, the gross MT organization in root epidermal cells appeared to be normal, indicating that these drugs might be influencing a MT function other than simple polymerization/depolymerization status. Taxol treatment of plant cells can also induce radial swelling without changing overall alignment of MT arrays (Weerderburg and Seagull, 1988; Baskin et al., 1994). Taxol and MT-depolymerizing drugs vinblastine and vincristine at their lowest effective concentrations appear to block mitosis in cultured mammalian cells by kinetically stabilizing spindle MTs and not by changing the mass of polymerized MTs (Jordan et al., 1993; Dhamdharan et al., 1995). Similarly, at concentrations that reportedly cause little change in the polymer level of MTs, taxol, vinblastine and another MT-depolymerizing drug, nocodazole, all dramatically decrease the rate of locomotion of fibroblasts, probably by suppressing MT dynamics (Liao et al., 1995). Therefore, it is possible that MT dynamics is also crucial in the function of the cortical array in plant cells and in proper anisotropic growth.

SPR1 and SPR2 may function in MT-dependent processes

Propyzamide and taxol affected the helical growth in *spr* seedlings. The most dramatic effect is exemplified in highly efficient suppression of almost isotropic cell expansion in the *spr1* hypocotyls and roots by low doses of these drugs. Moreover, *spr1* roots clearly responded to lower concentrations of MT-interacting drugs that did not visibly affect wild-type roots, by reducing their right-handed root skewing. Another feature of *spr1* phenotype is its temperature sensitivity: growth

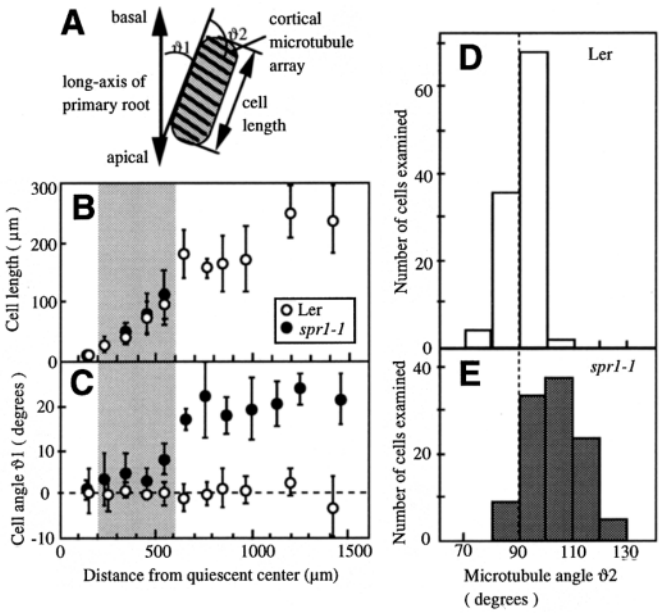

Fig. 10. Helical growth and orientation of cortical MT arrays in epidermal cells of seedling roots grown at 14°C. (A) Diagram illustrating the parameters measured in B-E. (B,C) Spatial profiles of cell length and skew angle (υ1) of Ler and *spr1-1* epidermal cells as a function of distance from the quiescent center. More than 300 cells representing more than 15 seedlings were measured for each genotype. (D,E) Distribution of MT angles (υ2) in epidermal cells located between 200 μm and 600 μm distal to the quiescent center (the region shaded in B and C). More than 100 cells representing 18 seedlings were measured for each genotype.

at 29°C tends to suppress the mutant phenotype, whereas growth at low temperatures exaggerates the phenotype. Cold destabilizes MTs and will lead to their depolymerization unless they are stabilized by associated proteins (Bokros et al., 1996). A large fraction of MT-related yeast mutants shows cold sensitivity (e.g. Richards et al., 2000). Collectively, these results suggest that *spr1* MTs are destabilized to some extent, or are defective in proper functioning in the tissues in which anisotropy is impaired.

spr2 seedlings show reduced response to the radial cell expansion effect of propyzamide, and increased response to the effect of taxol as compared to wild type. Although the *spr2* helical growth phenotype is not significantly altered by growth temperature, prolonged incubation of *spr2* seedlings at 4°C in the dark induces hair-like protrusions at the upper hypocotyl region (as in *spr1* epidermis under the same conditions), indicating that anisotropic growth of *spr2* epidermal cells is rendered somewhat cold-sensitive under certain conditions. Interestingly, transgenic *Arabidopsis* plants that overexpress a fusion protein between green-fluorescent protein and α-tubulin show anticlockwise arrangement of petals, cotyledons, and young rosette leaves in otherwise normal morphology and development, thus mostly phenocopying *spr2* (Ueda et al., 1999). Taken together, these data suggest that *spr2* disrupts an MT-dependent process as well. It should be noted, however, that *spr1* and *spr2* phenotypes are distinct in affected tissues, drug responses and cold sensitivity. The synergistic enhancement of anisotropic growth defects in the *spr1spr2* double mutant is in accordance with a model that *SPR1* and *SPR2* act on a similar process but in separate pathways in the control of MT-dependent anisotropic cell elongation.

Helical handedness

Drug-induced helical growth and the constitutive helical growth of *spr* mutants differ in their chirality; drug-induced helices are always left-handed, whereas helices in *spr1* and *spr2* mutants are invariably right-handed. Any model for helical growth needs to account for the fixed handedness. According to Fig. 11A, epidermal cells are predicted to exert a strong influence on the handedness. Although cellular defects in *spr1* are most obvious in ground tissue, epidermal cells under certain conditions show moderate radial swelling or local outgrowth of bulges, suggesting that the mutant epidermis has a compromised physical property and becomes partially defective in anisotropic growth under conditions that enhance the mutant phenotype. Likewise, low concentrations of propyzamide or taxol induce similar local bulges on the

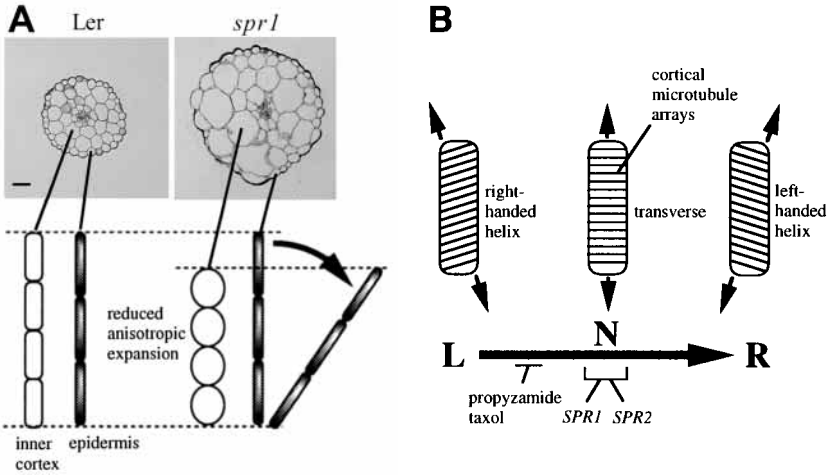

Fig. 11. (A) Model for helical growth. In the wild-type organ axis, the sum of inner cell length is equal to the sum of epidermal cell length, whereas inner cells of *spiral* mutant organs are defective in anisotropic growth and the total longitudinal length is shorter than that of epidermal cells. To compensate for this difference, the mutant epidermal cell files skew. The model also applies to the helical growth induced in wild-type seedlings by MT-interacting drugs. Cross sections of etiolated wild-type (Ler) and *spr1-1* hypocotyls are shown. (B) Model for helical handedness. Wild-type elongating epidermal cells are balanced in a neutral (N) state by the action between a pathway that shifts from a potential left-handed (L) state to a potential right-handed (R) state, and stabilizing (shown) or antagonistic pathways involving SPR1 and SPR2. The R-bound pathway is quantitatively suppressed by propyzamide or taxol. L and R states may represent elongating cells with compromised cortical MT arrays of right- or left-handed helix, respectively. The N cell with transverse arrays elongate perpendicular to the long axis but L and R cells skew respectively to the left and right during elongation.

hypocotyl epidermis of light-grown wild-type seedlings (T. H., unpublished). Here, we refer to the compromised state of epidermal cells that potentially give rise to a right-handed helical cell file as 'R', the opposite state as 'L', and the state that results in straight elongation parallel to the organ's long axis as 'N' (Fig. 11B). The R and L states may correspond to the cellular states before rapid elongation in which anisotropic cell expansion is partially impaired and may potentially give rise to a substantial loss of anisotropic expansion, as in the *spr1* ground tissue. The helical handedness induced by propyzamide or taxol suggests that intact dynamics of MTs pushes the state from L to N. Partial disruption of MT function by these drugs (possibly through suppression of dynamic instability) overrides the *spr* mutations, indicating that SPR1 and SPR2 function in the processes that prevent cells to proceed further from N to R in a MT-dependent pathway. SPR1 and SPR2 may represent a R-to-L reverse pathway, may act to suppress the L-to-R pathway or may stabilize the N state to prevent overshooting to R. Considering that the driving force for helical growth should come from radial swelling of inner cells and that elongating epidermis may function passively just to determine the direction of skewing, the difference between N and L, and between N and R are not necessarily large but should be consistent in a majority of elongating epidermal cells.

The orientation of cortical MT arrays in epidermal cells of L, N and R states showed right-handed helix (Z-helix), transverse and left-handed helix (S-helix), respectively. As studied in detail in the R state of *spr1* root epidermis, the helical pitch was not steep but of consistent handedness in a population of elongating cells. Assuming that the load-bearing innermost cellulose microfibrils are deposited along the helical MT arrays, the resulting microfibril arrangement on the outer tangential wall would then generate a polar cell growth in the direction perpendicular to the helical pitch of the arrays. Thus, a right-handed MT helical array in L is expected to give rise to left-handed helical growth, and a left-handed array in R would produce right-handed helical growth (Fig. 11B). If epidermal cells and neighboring cortex cells possess the same handedness of MT helix, a criss-cross cellulose microfibril pattern would be formed on the wall between them. The criss-cross pattern would seem to reduce the skewing force generated on that wall. In total, the helical pattern of the newly synthesized microfibrils on the outer wall of epidermis presumably has the strongest influence on the handedness of helical growth.

The model in Fig. 11B may be interpreted as a concept that the configurations of the cortical MT array can change from an S-helix to a Z-helix via transverse orientation, and that SPR1 and SPR2 act to partially suppress this transition. Oblique MTs are commonly observed in plant cells. In cases in which the handedness of helical arrays was studied, the orientation changes progressively from a flat S-helix to a steep Z-helix and then to a flat S-helix in differentiating tracheids (Abe et al., 1995), and the array in a given region of maize and arabidopsis root cells takes the same handedness, either an S- or Z-helix (Liang et al., 1996; Baskin et al., 1999). When MT orientation is synchronized in nonelongating epidermal cells of azuki bean epicotyls, the MT array can be induced to cycle between longitudinal and transverse via oblique orientation by treatments with plant hormones (Mayumi and Shibaoka, 1996; Takesue and Shibaoka, 1999). Reorientation can be suppressed when MTs are stabilized by taxol in differentiating tracheary elements (Falconer and Seagull, 1985). Thus, differentiation and a variety of internal and external stimuli appear to change the helical pitch and orientation of cortical MT arrays, and the *SPR* genes might be involved in some of these processes.

The model proposes that normal epidermal cells elongate parallel to the longitudinal axis of organs because SPR1 and SPR2 suppress the excess right-handed helical activity. Notably, wild-type arabidopsis roots of the ecotypes WS and Ler normally tend to bend somewhat to the left on a vertical agar surface, while seedling roots of Col ecotype grow almost straight to the gravity vector (Fig. 1A; Rutherford and Masson, 1996). A slight defect in MT function or somewhat stronger SPR activity in WS and Ler, compared with Col, might explain the observation. We also predict that tubulin mutations that partially compromise MT functions will cause left-handed helical growth and exaggerated left-slanting root growth on a vertical agar surface. Arabidopsis mutants with such a phenotype have been reported (Rutherford and Masson, 1996).

Helical growth model and circumnutation

Circumnutation is an oscillating growth pattern of plant axial organs that has attracted the attention of plant biologists since the era of Charles Darwin. A mechanistic model for circumnutation must explain the salient features of seedlings' circumnutational behavior (Brown, 1993). (1) Gravity is not required but can influence circumnutation. (2) Mechanical perturbations often have an immediate effect on the oscillations. (3) Circumnutations are absolutely growth dependent. Because circumnutation is clearly advantageous to the plant only in a small minority of cases (such as in twining plants) but is universally found in the plant kingdom, it is believed that some fundamental growth process underlies the behavior (Brown, 1993). Our MT-dependent helical growth model (Fig. 11) may explain circumnutation. The model is independent of gravity, but gravitropic responses of plant organs involve differential growth patterns on the convex and concave sides of the gravi-stimulated tissues (Hart, 1990), and thus are potentially capable of influencing the anisotropic expansion process. Mechanical forces imposed on a plant cell have been frequently implicated in having a profound influence on the alignment of cortical MTs (Cyr, 1994). Finally, the model is intrinsically growth dependent. The period of circumnutation considerably decreases at higher temperature (Johnsson, 1979). The proposed stabilization of MTs at higher temperature possibly stabilizes the N state, thereby decreasing the slanting angle of the elongating epidermis. Because a variety of plant hormones influences the organization of MTs (Shibaoka, 1994), physiological changes in cellular hormonal status may cause inconsistent oscillations of plant organs during extended periods of growth. In fact, the ethylene pathway strongly affects the helical phenotype in *spr1* mutant and the drug-treated seedlings (T. H., unpublished). A variation in the periodicity and handedness of circumnutation in a given plant has been well documented (Johnsson, 1979). It would be interesting to see whether circumnutation behavior is altered in *spr* mutants and in drug-treated seedlings.

We thank J. Schiefelbein and K. Nakamura for *spr1-2* and *spr1-3* alleles, respectively, and T. Schäffner for *tortifolia1*. We would like to acknowledge *Arabidopsis* Biological Resource Center for providing

convoluta seeds; K. Ueda, H. Tachimoto, K. Tuchihara, J. Uchida and K. Hayashi for technical assistance; and K. Sugimoto for assistance in immunostaining techniques. Helpful comments on the manuscript were kindly contributed by G. Wasteneys. This work was supported in part by Grants-in-Aid for Scientific Research on Priority Areas ('Molecular Mechanisms Controlling Multicellular Organization of Plant') for the Ministry of Education, Science, Sports and Culture, to T. H.

REFERENCES

Abe, H., Funada, R., Imaizumi, H., Ohtani, J. and Fukazawa, K. (1995). Dynamic changes in the arrangement of cortical microtubules in conifer tracheids during differentiation. *Planta* **197**, 418-421.

Baluska, F., Parker, J. S. and Barlow, P. W. (1992). Specific patterns of cortical and endoplasmic microtubules associated with cell growth and tissue differentiation in roots of maize (*Zea mays* L.). *J. Cell Sci.* **103**, 191-200.

Baluska, F., Parker, J. S. and Barlow, P. W. (1993). The microtubule cytoskeleton in cells of cold-treated roots of maize (*Zea mays* L.) shows tissue-specific responses. *Protoplasma* **172**, 84-96.

Baskin, T. I., Wilson, J. E., Cork, A. and Williamson, R. E. (1994). Morphology and microtubule organization in Arabidopsis roots exposed to oryzalin or taxol. *Plant Cell Physiol.* **35**, 935-942.

Baskin, T. I., Meekes, H. T. H. M., Liang, B. M. and Sharp, R. E. (1999). Regulation of growth anisotropy in well-watered and watered-stressed maize roots. II. Role of cortical microtubules and cellulose microfibrils. *Plant Physiol.* **119**, 681-692.

Beemster, G. T. S. and Baskin, T. I. (1998). Analysis of cell division and elongation underlying the developmental acceleration of root growth in *Arabidopsis thalinana*. *Plant Physiol.* **116**, 1515-1526.

Bokros, C. L., Hugdahl, J. D., Hanesworth, V. R., Murthy, J. V. and Morejohn, L. C. (1993). Characterization of the reversible taxol-induced polymerization of plant tubulin into microtubules. *Biochemistry* **32**, 3437-3447.

Bokros, C. L., Hugdahl, J. D., Blumenthal, S. D. and Morejohn, C. (1996). *Plant Cell Environ.* **19**, 539-548.

Brown, A. H. (1993). Circumnutations: from Darwin to space flights. *Plant Physiol.* **101**, 345-348.

Bürger, D. (1971). Die morphologischen Mutanten des Göttinger Arabidopsis-Sortiments, einschlieβlich der Mutanten mit abweichender Samenfarbe. *Arab. Inf. Serv.* **8**, 36-42.

Callos, J. D. and Medford, J. I. (1994). Organ positions and pattern formation in the shoot apex. *Plant J.* **6**: 1-7.

Capdevila, J., Vogan, K. J., Tabin, C. J. and Belmonte, J. C. I. (2000). Mechanisms of left-right determination in vertebrates. *Cell* **101**, 9-21.

Coen, E. (1999). In *The Art of Genes*, pp. 258-279. New York: Oxford University Press.

Cyr, R. J. (1994). Microtubule in plant morphogenesis: role of the cortical array. *Annu. Rev. Cell Biol.* **10**, 153-180.

Darwin, C. A. (1875). *The Movements and Habits of Climbing Plants*. London: John Murray.

Darwin, C. A. and Darwin, F. (1880). *The Power of Movement in Plants.* London: John Murray.

Dhamodharan, R., Jordan, M. A., Thrower, D., Wilson, L. and Wadsworth, P. (1995). Vinblastine suppresses dynamics of individual microtubules in living interphase cells. *Mol. Biol. Cell* **6**, 1215-1229.

Fabri, C. O. and Schäffner, A. R. (1994). An *Arabidopsis thaliana* RFLP mapping set to localize mutations to chromosome regions. *Plant J.* **5**, 149-156.

Falconer, M. M. and Seagull, R. W. (1985). Xylogenesis in tissue culture: taxol effects on microtubule reorientation and lateral association in differentiating cells. *Protoplasma* **128**, 157-166.

Gendreau, E., Traas, J., Desnos, T., Grandjean, O., Caboche, M. and Höfte, H. (1997). Cellular basis of hypocotyl growth in *Arabidopsis thaliana*. *Plant Physiol.* **114**, 295-305.

Giddings, T. H. Jr. and Staehelin, L. A. (1991). Microtubule-mediated control of microfibril deposition: A re-examination of the hypothesis. In *The Cytoskeletal Basis of Plant Growth and Form* (ed. C.W. Lloyd), pp. 85-100. San Diego: Academic.

Hasenstein, K. H., Blancaflor, E. B. and Lee, J. S. (1999). The microtubule cytoskeleton does not integrate auxin transport and gravitropism in maize roots. *Physiol. Plant.* **105**, 729-738.

Hart, J. W. (1990). *Plant Tropisms and Other Growth Movements*, pp. 74-82. London: Chapman & Hall.

Haughn, G. W. and Somerville, C. (1986). Sulfonylurea-resistant mutants of *Arabidopsis thaliana*. *Mol. Gen. Genet.* **204**, 430-434.

Johnsson, A. (1979). Circumnutation. In *Encyclopedia of Plant Physiology* (ed. W. Haupt and M.E. Feinleib), pp. 627-646. Berlin: Springer-Verlag.

Jordan, M. A., Toso, R. J., Thrower, D. and Wilson, L. (1993). Mechanism of mitotic block and inhibition of cell proliferation by taxol at low concentrations. *Proc. Natl. Acad. Sci. USA* **90**, 9552-9556.

Liang, B. M., Dennings, A. M., Sharp, R. E. and Baskin, T. I. (1996). Consistent handedness of microtubule helical arrays in maize and Arabidopsis primary roots. *Protoplasma* **190**, 8-15.

Liao, G., Nagasaki, T. and Gundersen, G. G. (1995). Low concentrations of nocodazole interfere with fibroblast locomotion without significantly affecting microtubule level: implications for the role of dynamic microtubules in cell locomotion. *J. Cell Sci.* **108**, 3473-3483.

Marinelli, B., Gomarasca, S. and Soave, C. (1997). A pleiotropic *Arabidopsis thaliana* mutant with inverted root chirality. *Planta* **202**, 196-205.

Mayumi, K. and Shibaoka, H. (1996). The cyclic reorientation of cortical microtubules on walls with a crossed polylamellate structure: effects of plant hormones and an inhibitor of protein kinases on the progression of the cycle. *Protoplasma* **195**, 112-122.

Morejohn, L. C. (1991). The molecular pharmacology of plant tubulin and microtubules. In *The Cytoskeletal Basis of Plant Growth and Form* (ed. C.W. Lloyd), pp. 29-43. San Diego: Academic.

Okada, K. and Shimura, Y. (1990). Reversible root tip rotation in *Arabidopsis* seedlings induced by obstacle-touching stimulus. *Science* **250**, 274-276.

Relichova, J. (1976). Some new mutants. *Arab. Inf. Serv.* **13**, 25-28.

Richards, K. L., Anders, K. R., Nogales, E., Schwartz, K., Downing, K. H. and Botstein, D. (2000). Structure-function relationships in yeast tubulins. *Mol. Biol. Cell* **11**, 1887-1903.

Rutherford, R. and Masson, P. H. (1996). *Arabidopsis thaliana sku* mutant seedlings show exaggerated surface-dependent alteration in root growth vector. *Plant Physiol.* **111**, 987-998.

Scheres, B., Wokenfelt, H., Willemsen, V., Terlouw, M., Lawson, E., Dean, C. and Weisbeek, P. (1994). Embryonic origin of the *Arabidopsis* primary root and root meristem initials. *Development* **120**, 2475-2487.

Shibaoka, H. (1994). Plant hormone-induced changes in the orientation of cortical microtubules: alterations in the cross-linking between microtubules and the plasma membrane. *Annu. Rev. Plant Physiol. Plant Mol. Biol.* **45**, 527-544.

Simmons, C., Söll, D. and Miglicaccio, F. (1995). Circumnutation and gravitropism cause root waving in *Arabidopsis thaliana*. *J. Exp. Bot.* **46**, 143-150.

Takesue, K. and Shibaoka, H. (1999). Auxin-induced longitudinal-to-transverse reorientation of cortical microtubules in nonelongating epidermal cells of azuki bean epicotyls. *Protoplasma* **206**, 27-30.

Ueda, K., Matsuyama, T. and Hashimoto, T. (1999). Visualization of microtubules in living cells of transgenic *Arabidopsis thaliana*. *Protoplasma* **206**, 201-206.

Wasteneys, G. O., Sugimoto, K. and Baskin, T. (1998). Comparison of fixation methods for analysis of a plant microtubule mutant. *Cell Biol. Intl.* **21**, 905-907.

Weerderburg, C. and Seagull, R. W. (1988). The effects of taxol and colchicine on microtubule and microfibril arrays in elongating plant cells in culture. *Can J. Bot.* **66**, 1707-1716.

Williams, R. F. (1975). *The Shoot Apex and Leaf Growth*. London: Cambridge University Press.

Woodrick, R., Martin, P. R., Birman, I. and Pickett, F. B. (2000). The *Arabidopsis* embryonic shoot fate map. *Development* **127**, 813-820.